High-Temperature Corrosion And Materials Applications
George Y. Lai, editor, p409-421
DOI: 10.1361/hcma2007p409

CHAPTER 15

Molten Salt Corrosion

15.1 Introduction

Molten salt technology plays an important role in various industries. In the heat treating industry, molten salts are commonly used as a medium for heat treatment of metals and alloys (e.g., annealing, tempering, hardening, quenching, and cleaning) as well as for surface treatment (e.g., case hardening). In nuclear and solar energy systems, they have been used as a medium for heat transfer and energy storage. Other applications include extraction of aluminum, magnesium, sodium, and other reactive metals; refining of refractory metals; and high-temperature batteries and fuel cells. Table 15.1 summarizes the general applications of molten salt technology in several industries (Ref 1).

The containment material, which is in contact with the molten salt, is subject to molten salt corrosion. This chapter reviews the data relevant to the corrosion of containment materials. Although the literature related to studies of corrosion in molten salts is extensive, as can be seen in an annotated bibliography prepared by Janz and Tomkins (Ref 2), corrosion data useful in selecting materials are rather limited and fragmented.

15.2 Corrosion Process

Molten salts generally are a good fluxing agent, effectively removing oxide scales from a metal surface. The corrosion reaction proceeds primarily by oxidation, which is then followed by dissolution of metal oxides in the melt. Oxygen and water vapor in the molten salt thus often accelerate molten salt corrosion.

Corrosion can also take place through mass transfer due to thermal gradient in the melt. This mode of corrosion involves dissolution of an alloying element at hot spots and deposition of that alloying element at cooler spots. This can result in severe fouling and plugging in a circulating system. Corrosion is also strongly dependent on temperature and velocity of the salt.

Corrosion can take the form of uniform thinning, pitting, or internal or intergranular attack. In general, molten salt corrosion is quite similar to aqueous corrosion. More complete discussion on the mechanisms of molten salt corrosion can be found in Ref 3 to 5.

15.3 Corrosion in Molten Chlorides

Chloride salts are widely used in the heat treating industry for annealing and normalizing of steels. These salts are commonly referred to as neutral salt baths. The most common neutral salt baths are barium, sodium, and potassium chlorides, used separately or in combination in the temperature range of 760 to 980 °C (1400 to

Table 15.1 General applications of molten salt technology in several industries

Power	Metals/materials	Chemicals
Solar/thermal: collection, storage, transfer	Extraction: refractory metals, actinides, lanthanides, transition, and light metals	Fuels: cracking, catalysts
Nuclear: homogeneous reactors, reprocessing	Processing: heat treatment, annealing, quenching, cleaning, cementation, electroforming	Plastics: curing, etching, vulcanizing
Batteries	Surface finishing: anodizing, plating	Pyrolysis: recycling, scrap treatment, hazardous materials disposal
Fuel cells	Joining: fluxes and slags for welding, brazing, soldering, and electroslag refining	Synthesis: organics, gases
	Composites: glasses, ceramics, slags	Special applications: liquid crystals, single-crystal growing, matrix
	Recycling	

Source: Ref 1

1800 °F). Compositions of some common neutral salt baths are (Ref 6):

- 50NaCl-50KCl
- 50KCl-50Na_2CO_3
- 20NaCl-25KCl-55$BaCl_2$
- 25NaCl-75$BaCl_2$
- 21NaCl-31$BaCl_2$-48$CaCl_2$

Jackson and LaChance (Ref 6) performed an extensive study on the corrosion of cast Fe-Ni-Cr alloys in the NaCl-KCl-$BaCl_2$ salt bath. They found that alloys suffered intergranular attack more than metal loss. Corrosion data in terms of metal loss and intergranular attack are shown in Fig. 15.1 and 15.2, respectively. The figures also indicate that resistance to the molten salt (NaCl-KCl-$BaCl_2$) increases with decreasing chromium and increasing nickel in Fe-Ni-Cr alloys. HW alloy (Fe-12Cr-60Ni) was consistently the best performer among the four commercial cast alloys (HW, HT, HK, and HH alloys) studied. These authors further noted that intergranular attack generally followed grain-boundary carbides. Thus, lowering carbon from 0.4% to about 0.07% resulted in a threefold improvement. Decreasing grain size also improved alloy resistance to intergranular attack. Five different neutral salt baths were compared for HW, HT, and three Fe-Cr alloys, as shown in Fig. 15.3. In general, the four chloride salt baths were quite similar. The KCl-Na_2CO_3 salt bath was significantly less aggressive than pure chloride baths. It is also interesting to note that Fe-17Cr alloy was better than HW (Fe-12Cr-60Ni) and HT (Fe-15Cr-35Ni) alloys in NaCl-KCl, NaCl-KCl-$BaCl_2$, and NaCl-$BaCl_2$-$CaCl_2$ salt baths.

Lai et al. (Ref 7) evaluated various wrought iron-, nickel-, and cobalt-base alloys in a NaCl-KCl-$BaCl_2$ salt bath at 840 °C (1550 °F) for 1 month (Fig. 15.4). Surprisingly, two high-nickel alloys (alloys 600 and 601) suffered more corrosion attack than stainless steels such as Types 304 and 310. Co-Ni-Cr-W, Fe-Ni-Co-Cr, and Ni-Cr-Fe-Mo alloys performed best. Laboratory testing in a simple salt bath failed to reveal the correlation between alloying elements

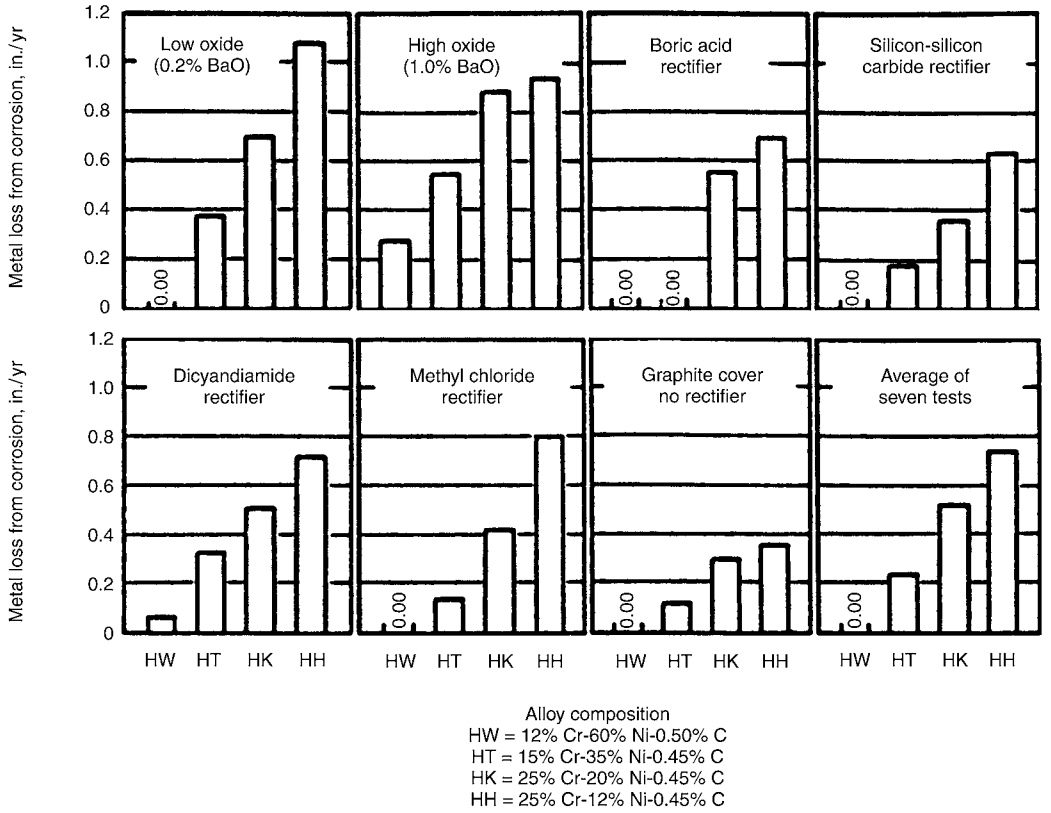

Fig. 15.1 Corrosion rates in terms of metal loss for four commercial cast Fe-Ni-Cr alloys in a 20NaCl-25KCl-55$BaCl_2$ salt bath under different conditions of rectification at 870 °C (1600 °F) for 60 h. Source: Ref 6

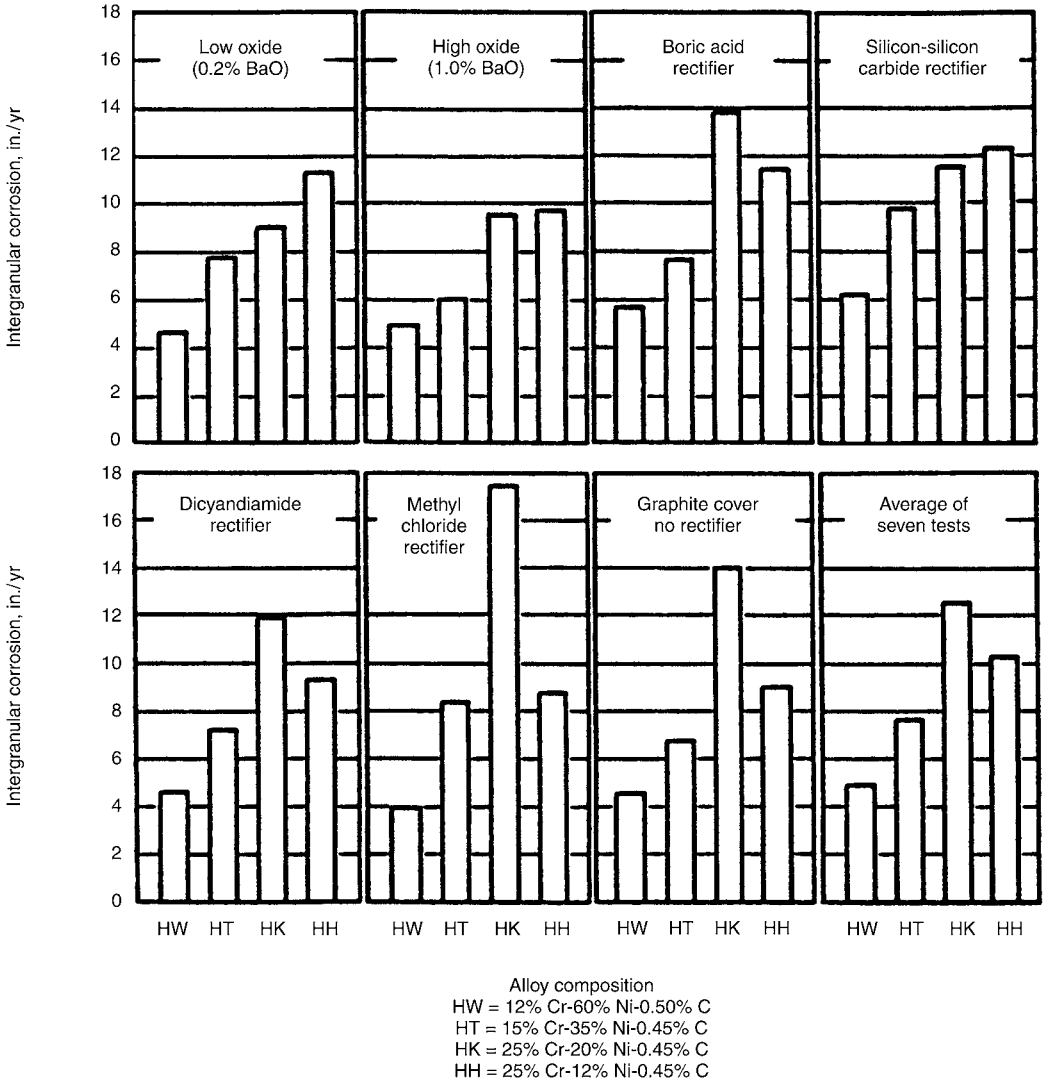

Fig. 15.2 Corrosion rates in terms of intergranular attack for four commercial cast Fe-Ni-Cr alloys in a 20NaCl-25KCl-55$BaCl_2$ salt bath under different conditions of rectification at 870 °C (1600 °F) for 60 h. Source: Ref 6

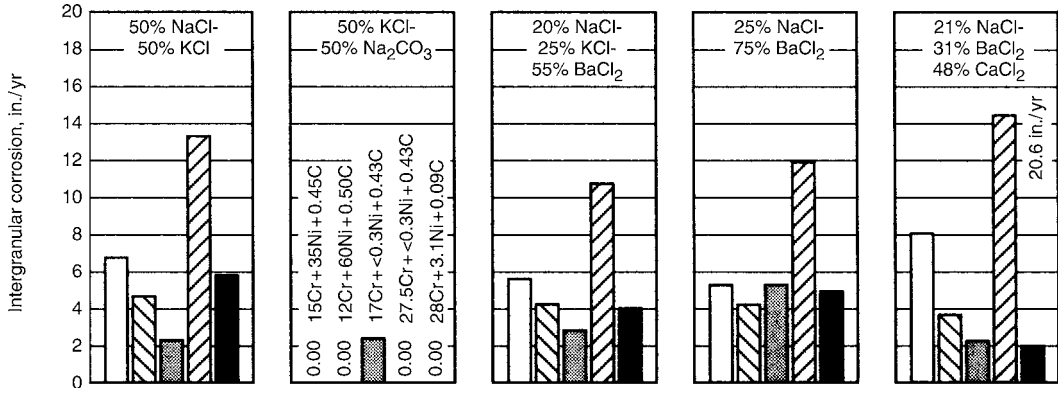

Fig. 15.3 Comparison of different neutral salt baths for HW, HT, and Fe-Cr alloys at 870 °C (1600 °F) for 60 h. Source: Ref 6

and performance. Tests were conducted at 840 °C (1550 °F) for 100 h in a NaCl salt bath with fresh salt for each test run. Results are tabulated in Table 15.2 (Ref 7, 8). Similar to the field test results, Co-Ni-Cr-W and Fe-Ni-Co-Cr alloys performed best.

Evaluating a eutectic sodium-potassium-magnesium chloride (33NaCl-21.5KCl-45.5$MgCl_2$, mol%) as a possible heat-transfer and energy-storage medium in solar thermal energy systems for power generation, Coyle et al. (Ref 9) conducted corrosion tests on various commercial alloys at 900 °C (1650 °F) for 144 and 456 h

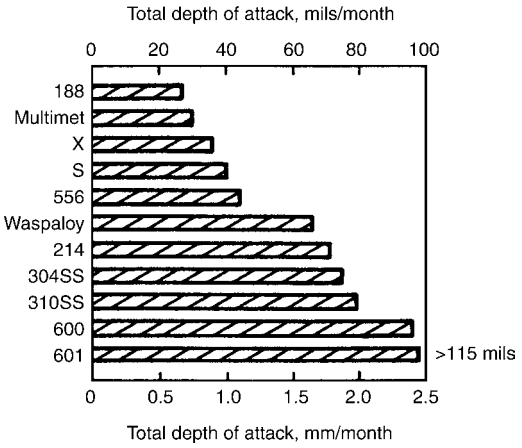

Fig. 15.4 Results of a field rack test in a NaCl-KCl-$BaCl_2$ salt bath at 840 °C (1550 °F) for 1 month. Source: Ref 7

Table 15.2 Results of laboratory tests in a NaCl salt bath at 840 °C (1550 °F) for 100 h

Alloy	Total depth of attack(a), mm (mils)
188	0.051 (2.0)
25	0.064 (2.5)
556	0.066 (2.6)
601	0.066 (2.6)
Multimet	0.069 (2.7)
150	0.076 (3-0)
214	0.079 (3.1)
304	0.081 (3.2)
446	0.081 (3.2)
316	0.081 (3.2)
X	0.097 (3.8)
310	0.107 (4.2)
800H	0.109 (4.3)
625	0.112 (4.4)
RA330	0.117 (4.6)
617	0.122 (4.8)
230	0.140 (5.5)
S	0.168 (6.6)
RA330	0.191 (7.5)
600	0.196 (7.7)

A fresh salt bath was used for each test run; air was used for the cover gas. (a) Mainly intergranular attack; no metal wastage. Source: Ref 7 and 8

(Table 15.3). Fifteen alloys, including iron-, nickel-, and cobalt-base alloys, were evaluated. After 144 h of exposure, specimens of eight alloys were consumed. The remaining seven alloys disintegrated after 456 h of exposure. The authors concluded that the chloride salt was too aggressive to be used at 900 °C (1650 °F).

At lower temperatures, molten salts generally become less aggressive. Susskind et al. (Ref 10) conducted corrosion tests at 450 to 500 °C (840 to 930 °F) in molten NaCl-KCl-$MgCl_2$ eutectic and found many alloys resistant to molten salt corrosion (Table 15.4). Low corrosion rates may also be attributed to the vacuum environment used in these tests. Investigating the corrosion behavior of alloys at 400 and 500 °C

Table 15.3 Results of corrosion tests in molten eutectic NaCl-KCl-$MgCl_2$ salt at 900 °C (1650 °F)

	Weight change, mg/cm^2	
Alloy	144 h	456 h
304	Disintegrated	…
316	Disintegrated	…
800	Disintegrated	…
800H	−310	Disintegrated
556	−250	Disintegrated
Nickel	Disintegrated	…
600	−280	Disintegrated
214	−120	Disintegrated
X	Disintegrated	…
N	Disintegrated	…
S	−400	Disintegrated
230	−300	Disintegrated
X-750	Disintegrated	…
R-41	−150	Disintegrated
188	Disintegrated	…

N_2-(0.1–1H_2O)-(1–10O_2) was used for the cover gas. Source: Ref 9

Table 15.4 Corrosion of alloys in molten eutectic NaCl-KCl-$MgCl_2$ salt at 450 to 500 °C (840 to 930 °F) with 50 °C temperature differential under vacuum for 1000 h

Alloy	Maximum penetration, mm/yr (mpy)
1020	0
2.25Cr-lMo	0.08 (3)
304	<0.01 (0.4)
310	0
316	<0.01 (0.4)
347	0.12 (4.7)
410	0.03 (1.0)
430	0.05 (2)
446	<0.01 (0.4)
600	0.05 (1.8)
N	0.05 (2)
Molybdenum	0
Tantalum	0.07 (2.9)

Source: Ref 10

(750 and 930 °F) in the molten LiCl-KCl eutectic, which was being considered as an electrolyte for lithium-sulfur fuel cells, Battles et al. (Ref 11) also found many alloys resistant to molten salt (Table 15.5). Tests were conducted in closed quartz crucibles. All the alloys tested showed negligible corrosion rates. Aluminum in the aluminum-clad Type 434 SS sample corroded at a higher rate due to the galvanic couple between aluminum and stainless steel (Ref 11).

Takehara and Ueshiba (Ref 12) investigated the corrosion behavior of steel, Fe-Cr, Fe-Ni, and Fe-Cr-Ni alloys in molten 20NaCl-30$BaCl_2$-50$CaCl_2$ and molten 25LiCl-25$ZnCl_2$-16$BaCl_2$-24$CaCl_2$-10NaCl at 500 and 600 °C (930 and 1100 °F). It was not clear what type of cover gas was involved in these tests. The results from both salt mixtures are summarized in Fig. 15.5 and 15.6. Steels and Fe-Cr alloys suffered severe corrosion in both types of salts. Chromium in Fe-Cr alloys and nickel in Fe-Ni alloys improved performance. Fe-Cr-Ni alloys performed significantly better than steels and Fe-Cr alloys.

Intergranular corrosion is the major corrosion morphology by molten chloride salts. Figures 15.7 and 15.8 show typical intergranular corrosion by molten chloride salt. Figure 15.7 shows the intergranular attack of a Ni-Cr-Fe alloy (alloy 600) coupon welded to a heat treat basket that underwent heat treat cycles involving

Table 15.5 Corrosion rates of several metals and alloys in molten LiCl-KCl eutectic

	Corrosion rate, µm/yr (mpy)			
	Annealed samples		Sensitized samples(a)	
Material	400 °C (750 °F)	500 °C (930 °F)	400 °C (750 °F)	500 °C (930 °F)
304	2 (0.08)	6 (0.24)	3 (0.12)	5 (0.2)
316	2 (0.08)	…	…	…
347	…	2 (0.08)	1 (0.04)	1 (0.04)
430	2 (0.08)	…	…	…
E-Brite	8 (0.32)	6 (0.24)	4 (0.16)	5 (0.2)
Al-Clad Type 434	130 (5.1)	…	…	…
Iron (99.999% Fe)	41 (1.6)	…	…	…
Armco electromagnet iron	12 (0.47)	…	…	…

Tests were conducted in closed quartz crucibles. (a) Samples were sensitized at 650 °C (1200 °F) for 120 h. Source: Ref 11

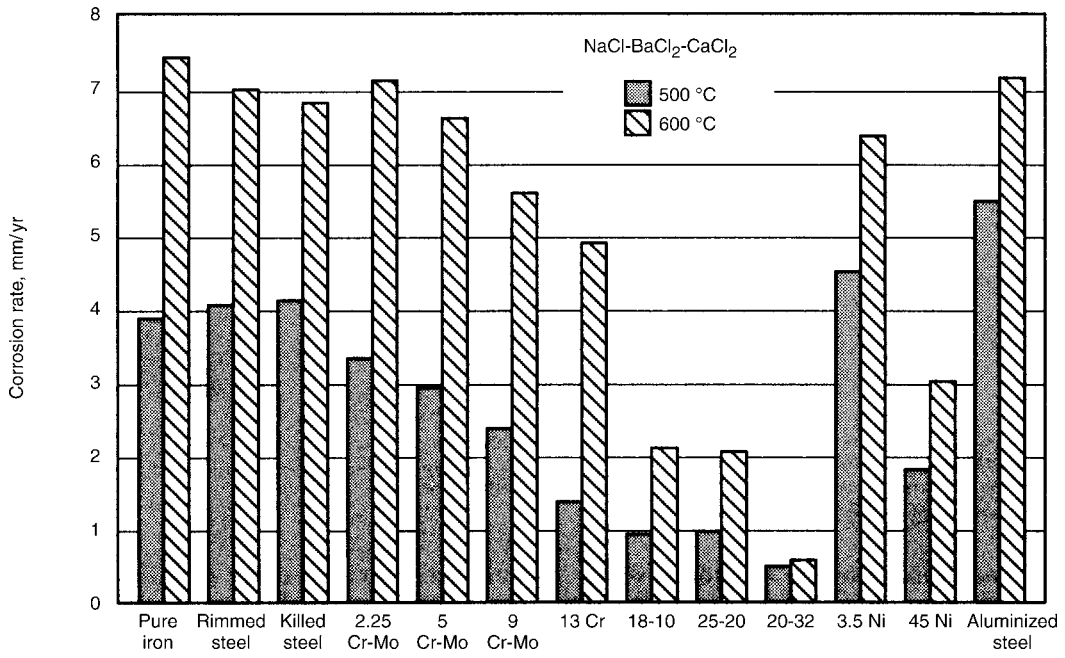

Fig. 15.5 Corrosion rates of steel, Fe-Cr, Fe-Ni, and Fe-Cr-Ni alloys in molten 20NaCl-30$BaCl_2$-50$CaCl_2$ at 500 and 600 °C (930 and 1110 °F). Source: Ref 12

a molten KCl salt bath at 870 °C (1600 °F) and a quenching salt bath of molten sodium nitrate and sodium nitrite at 430 °C (800 °F) for 1 month (Ref 13). Figure 15.8 shows the intergranular attack of a heat treat basket made of the same alloy after service for 6 months in the same heat treat cycling operation (Ref 13).

Another frequently observed corrosion morphology is internal attack by void formation (Fig. 15.9) (Ref 13). Voids tend to form at grain boundaries as well as in the grain interior (Ref 4). The continuing formation and growth of chromium compounds at the metal surface causes outward migration of chromium and inward migration of vacancies, thus leading to internal void formation (Ref 4).

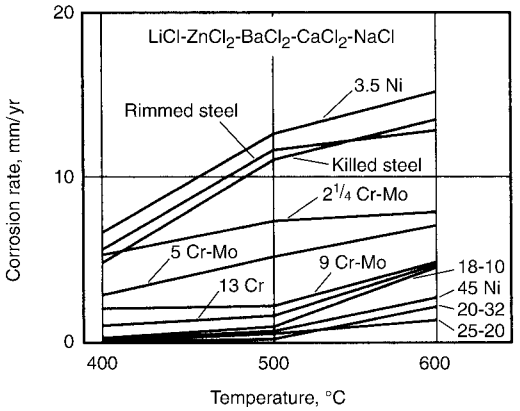

Fig. 15.6 Corrosion rates of steel, Fe-Cr, Fe-Ni, and Fe-Cr-Ni alloys in molten 25LiCl-25$ZnCl_2$-16$BaCl_2$-24$CaCl_2$-10NaCl at 500 and 600 °C (930 and 1110 °F). Source: Ref 12

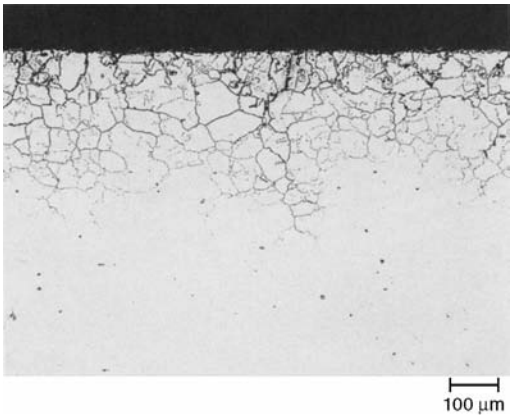

Fig. 15.7 Intergranular attack of a Ni-Cr-Fe alloy coupon welded to a heat treat basket after service for 1 month in a heat treat operation cycling between a molten KCl bath at 870 °C (1600 °F) and a quenching salt bath of molten sodium nitrate-nitrite at 430 °C (800 °F). Source: Ref 13

Cold work may significantly affect corrosion of alloys in molten chloride salts. Lai (Ref 14) discovered severe intergranular corrosion at the sheared edge of a Ni-Cr-Fe-Mo alloy (alloy X) coupon after exposure in a molten $CaCl_2$-NaCl salt bath at 570 °C (1050 °F). The sample edge

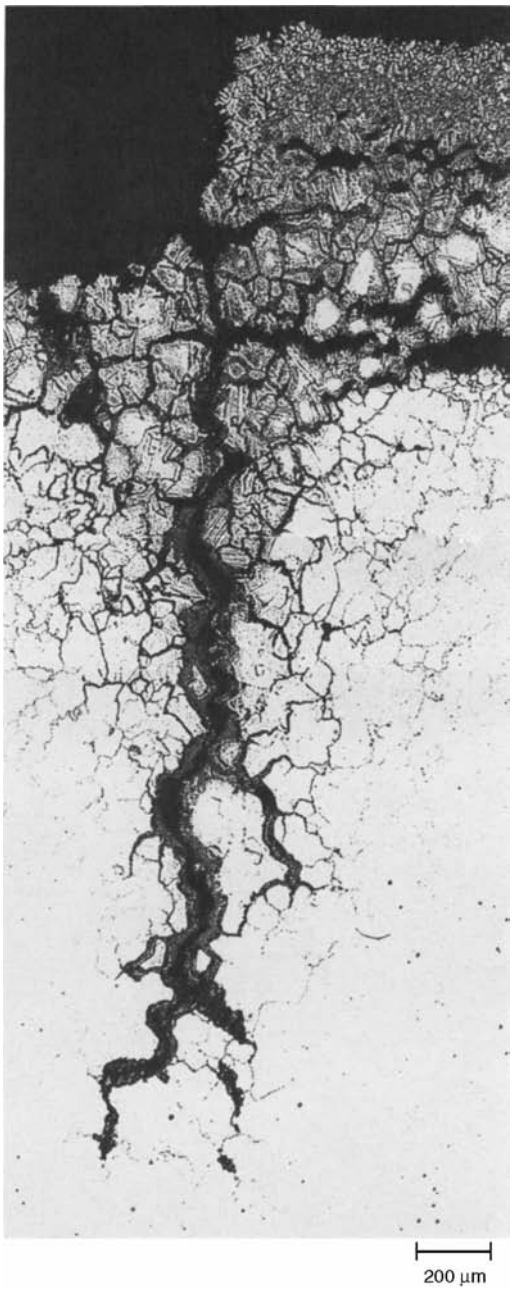

Fig. 15.8 Intergranular attack of a Ni-Cr-Fe alloy heat treat basket after service for 6 months in the same heat treat cycling operation described in Fig. 15.7. Source: Ref 13

was cold worked during sample shearing prior to exposure. There was no evidence of intergranular corrosion in the area away from the sheared edge (Fig. 15.10). The prior cold work also resulted in a thicker oxide scale during exposure in the molten salt. A Co-Ni-Cr-W alloy (alloy 188) exhibited similar behavior.

15.4 Corrosion in Molten Nitrates/ Nitrides

Molten nitrates or nitrate-nitride mixtures are widely used for heat treat salt baths, typically operating from 160 to 590 °C (325 to 1100 °F). They are also used as a medium for heat transfer or energy storage. Molten drawsalt ($NaNO_3$-KNO_3) is being considered as a heat-transfer and energy-storage medium for a solar central receiver for power generation from solar energy. Numerous studies (Ref 15–21) have been carried out to determine potential candidate containment materials for handling molten drawsalt. Bradshaw and Carling (Ref 22) recently summarized these studies as well as the results of their study (Table 15.6) (Ref 22). The data suggest that, for temperatures up to 630 °C (1170 °F), many alloys are adequate for handling molten $NaNO_3$-KNO_3 salt. Carbon steel and 2.25Cr-1Mo steel exhibited low corrosion rates (<0.13 mm/yr, or <5 mpy) at 460 °C (860 °F). At 500 °C (932 °F), 2.25Cr-1Mo steel exhibited a corrosion rate of about 0.026 mm/yr (1 mpy). Aluminized Cr-Mo steel showed higher resistance, with a corrosion rate of less than 0.004 mm/yr (<0.2 mpy) at 600 °C (1110 °F). Austenitic stainless steels, alloy 800, and alloy 600 were more resistant than carbon steel and Cr-Mo steels. Nickel, however, suffered high corrosion rates.

Slusser et al. (Ref 23) evaluated the corrosion behavior of a variety of alloys in molten $NaNO_3$-KNO_3 (equimolar volume) salt with an equilibrium nitrite concentration (about 6 to 12 wt%) at 675 °C (1250 °F) for 336 h. A

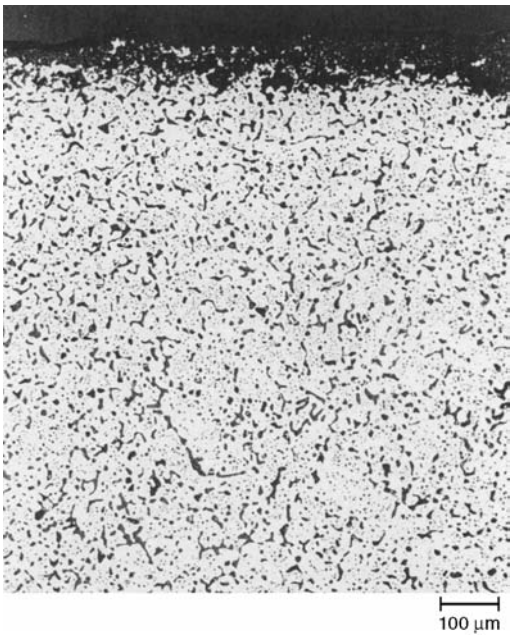

Fig. 15.9 Corrosion attack consisting of voids in a nickel-base alloy after 2 months at 870 °C (1600 °F) in a molten $BaCl_2$ salt bath. Source: Ref 13

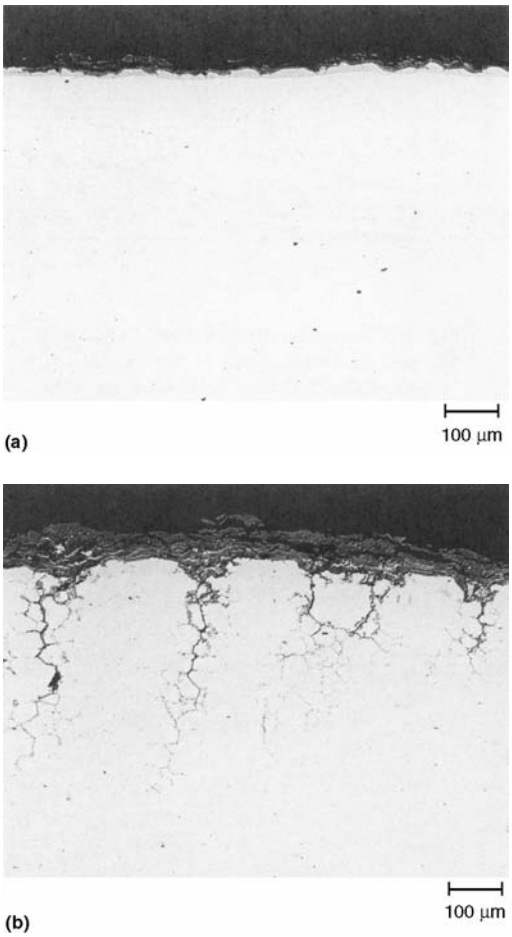

Fig. 15.10 Corrosion of Ni-Cr-Fe-Mo alloy in a molten $CaCl_2$-NaCl salt bath at 570 °C (1050 °F) for 6 months. (a) Little corrosion at the area not cold worked (away from the sheared edge). (b) Intergranular attack at the cold worked area (specimen sheared edge). Source: Ref 14

constant purge of air in the melt was maintained during testing. Nickel-base alloys were generally much more resistant than iron-base alloys. Increasing nickel content improved alloy corrosion resistance to molten nitrate-nitrite salt. However, pure nickel suffered rapid corrosion attack. Figure 15.11 shows the corrosion rates of various alloys as a function of nickel content (Ref 23). Silicon-containing alloys, such as RA330 and Nicrofer 3718, performed poorly. A long-term test (1920 h) at 675 °C (1250 °F) was performed on selected alloys, showing corrosion rates similar to those obtained from 336 h exposure tests (Table 15.7). Alloy 800, however, exhibited a higher corrosion rate in the 1920 h test than in the 336 h test. As the temperature was increased to 700 °C (1300 °F), corrosion rates became much higher, particularly for iron-base alloy 800, which suffered an unacceptably high corrosion rates (Table 15.7). Boehme and Bradshaw (Ref 24) attributed the increased corrosion rate with increasing temperature to higher alkali oxide concentration. Slusser et al. (Ref 23) found that adding sodium peroxide (Na_2O_2) to the salt increased the salt corrosivity.

15.5 Corrosion in Molten Sodium Hydroxide (Caustic Soda)

The reaction of metals with molten sodium hydroxide (NaOH) leads to metal oxide, sodium oxide, and hydrogen (Ref 25). Nickel is most resistant to molten NaOH (Ref 26–29), particularly low-carbon nickel such as Ni 201 (Ref 30). Gregory et al. (Ref 29) reported corrosion rates of several nickel-base alloys obtained from static tests at 400 to 680 °C (750 to 1256 °F) (Table 15.8). Molybdenum and silicon appear to be detrimental alloying elements in molten NaOH salt. Iron may also be detrimental. Molybdenum and iron were found to be selectively removed from nickel-base alloys with less than 90% nickel, leading to the formation of internal voids (Ref 31).

Molten sodium hydroxide becomes increasingly aggressive with increasing temperature. Coyle et al. (Ref 9) evaluated a variety of alloys for a possible containment material for molten sodium hydroxide operating at 900 °C (1650 °F) for a solar power generation system. Test results are tabulated in Table 15.9. Many

Table 15.6 Corrosion rates of selected metals and alloys in molten $NaNO_3$-KNO_3

Alloy	Temperature °C (°F)	Corrosion rate, mm/yr (mpy)
Carbon steel	460 (860)	0.120 (4.7)
2.25Cr-lMo	460 (860)	0.101 (4.0)
	500 (932)	0.026 (1.0)
9Cr-lMo	550 (1020)	0.006 (0.2)
	600 (1110)	0.023 (0.9)
Aluminized Cr-Mo steel	600 (1110)	<0.004 (0.2)
12Cr steel	600 (1110)	0.022 (0.9)
304SS	600 (1110)	0.012 (0.5)
316SS	600 (1110)	0.007–0.010 (0.3–0.4)
	630 (1170)	0.106 (4.2)
800	565 (1050)	0.005 (0.2)
	600 (1110)	0.006–0.01 (0.2–0.4)
	630 (1170)	0.075 (3.0)
600	600 (1110)	0.007–0.01 (0.3–0.4)
	630 (1170)	0.106 (4.2)
Nickel	565 (1050)	>0.5 (20)
Titanium	565 (1050)	0.04 (1.6)
Aluminum	565 (1050)	<0.004 (0.2)

Source: Ref 22

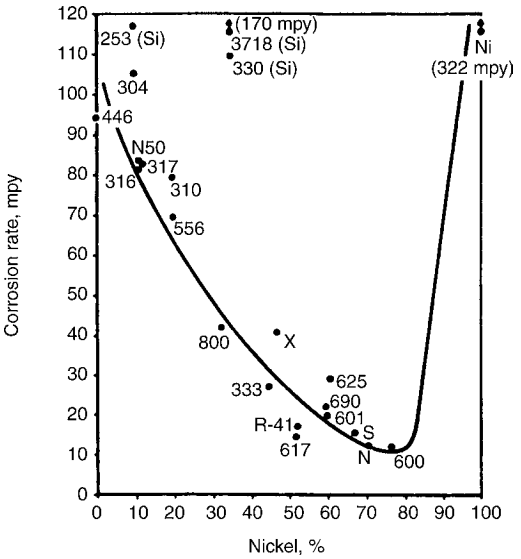

Fig. 15.11 Corrosion rates of various alloys as a function of nickel content in the alloy tested in molten $NaNO_3$-KNO_3 salt at 675 °C (1250 °F). Source: Ref 23

Table 15.7 Corrosion rates of selected alloys at 675 and 700 °C (1250 and 1300 °F) in sodium-potassium nitrate-nitrite salt

Alloy	Corrosion rate, mm/yr (mpy)	
	675 °C (1250 °F) 1920 h	700 °C (1300 °F) 720 h
214	0.41 (16)	0.53 (21)
600	0.25 (10)	0.99 (39)
N	0.23 (9.1)	1.22 (48)
601	0.48 (19)	1.25 (49)
800	1.85 (73)	6.6 (259)

Source: Ref 23

iron-, nickel-, and cobalt-base alloys disintegrated in 84 h. Samples of the alloys that survived the 84 h exposure test were severely corroded. Scales that formed on these samples were reportedly cracked and spalled. The weight-gain or weight-loss data of surviving samples were no longer indicative of alloy performance ranking. No metallographic examination was performed on these samples. The authors concluded that no further studies on molten sodium hydroxide were necessary, because the salt was too aggressive to metallic materials operating at 900 °C (1650 °F). The marked influence of temperature on the corrosiveness of molten sodium hydroxide is also demonstrated by the results shown in Table 15.10 (Ref 26).

Corrosion of metals and alloys in molten NaOH depends strongly on the velocity of the salt. Gregory et al. (Ref 32) showed that corrosion of nickel under dynamic conditions was enhanced by as much as several times at 540 °C (1000 °F) and higher. The corrosion rate for nickel at 680 °C (1250 °F), for example, varied from about 1 mm/yr (40 mpy) under static conditions to about 8 mm/yr (320 mpy) at a rotational speed of 600 rpm (Ref 32).

Metals or alloys in molten sodium hydroxide are susceptible to mass transfer due to thermal gradients in the melt. This causes corrosion in the hot zone, and potential tube plugging in the cold zone, of a circulating system. For example, 6.35 mm (0.25 in.) nickel tubing was plugged after 5000 h at 440 to 480 °C (830 to 900 °F), and after 50 h at 690 to 730 °C (1280 to 1350 °F) (Ref 27).

15.6 Corrosion in Molten Fluorides

Corrosion of alloys in molten fluoride salts has been extensively studied for nuclear reactor applications. The molten salt nuclear reactor uses a LiF-BeF_2 base salt as a fuel salt, containing various amounts of UF_4, ThF_4, and ZrF_4 (Ref 33). The reactor coolant salt is a $NaBF_4$-NaF mixture (Ref 33). A nickel-base alloy, Hastelloy alloy N, has proved to be the most corrosion resistant in molten fluoride salts (Ref 34). The

Table 15.8 Corrosion rates of selected nickel-base alloys obtained from static tests in molten sodium hydroxide

Alloy	Corrosion rate, mm/yr (mpy)			
	400 °C (750 °F)	500 °C (930 °F)	580 °C (1080 °F)	680 °C (1260 °F)
Ni-201	0.023 (0.9)	0.033 (1.3)	0.06 (2.5)	0.96 (37.8)
C	…	2.54 (100)	(a)	…
D	0.018 (0.7)	0.056 (2.2)	0.25 (9.9)	(a)
400	0.046 (1.8)	0.13 (5.1)	0.45 (17.6)	…
600	0.028 (1.1)	0.06 (2.4)	0.13 (5.1)	1.69 (66.4)
301SS	0.043 (1.7)	0.08 (3.2)	0.26 (10.4)	1.03 (40.7)
75	0.028 (1.1)	0.36 (14.3)	0.53 (20.8)	1.21 (47.6)

(a) Severe corrosion. Source: Ref 29

Table 15.9 Results of corrosion tests in molten sodium hydroxide at 900 °C (1650 °F) for 84 h

Alloy	Weight change, mg/cm^2
304	Disintegrated
316	Disintegrated
800	+60
800H	+65
556	Disintegrated
Nickel	−50
600	−27
214	+160
X	+22
N	Fractured
S	4
230	Disintegrated
X-750	+35
R-41	Disintegrated
188	Disintegrated

N_2-(0.1–1H_2O)-(1–10O_2) was used for the cover gas. Source: Ref 9

Table 15.10 Corrosion of various metals and alloys in molten sodium hydroxide

Material	Weight change rate(a), mg/cm^2-day	
	538 °C (1000 °F)	816 °C (1500 °F)
Ni-201	+0.12	+1.7
Copper	+1.54	−2.2
Chromium	−0.12	−40
Aluminum	−0.34	…
Silver	+0.02	+2.9
Gold	−0.33	Broke
Platinum	−0.32	Broke
70Au-30Pt	+0.36	Broke
Palladium	+6.59	+175
Colmonoy No. 5	+0.63	+70
Colmonoy No. 6	−0.48	−72
Colmonoy No. 9	−0.23	Dissolved in 24 h
Chromel P	+0.09	Dissolved in 24 h
Zirconium	+0.56	…

(a) Based on 24 h exposure tests. Source: Ref 26

alloy was the primary containment material for a molten salt test reactor successfully operated from 1965 to 1969 (Ref 35). Koger (Ref 33) reported a corrosion rate of less than 0.0025 mm/yr (0.1 mpy) at 704 °C (1300 °F) in the LiF-BeF_2 base salt (fuel salt) and about 0.015 mm/yr (0.6 mpy) at 607 °C (1125 °F) in the $NaBF_4$-NaF coolant salt for alloy N.

Iwamoto et al. (Ref 36) performed corrosion tests in eutectic LiF-NaF-KF salt in a test loop with a 750 °C (1380 °F) hot leg and a 685 °C (1265 °F) cold leg for 500 h. Alloy N exhibited only 2.06 mg/cm^2 of maximum weight loss at the hot leg.

At lower temperatures, austenitic stainless steels showed good performance. Type 316 exhibited 0.015 mm/yr (0.59 mpy) at 650 °C (1200 °F) in 66LiF-34BeF_2 (mol%), and about 0.002 mm/yr (0.08 mpy) at 530 °C (986 °F) in 22LiF-31LiCl-47LiBr (mol%) (Ref 37). In a LiF-BeF_2 fuel salt containing UF_4, ThF_4, and ZrF_4, Type 304 suffered a corrosion rate of only about 0.028 mm/yr (1.1 mpy) at 690 °C (1270 °F) (Ref 33).

Corrosion can become more aggressive as temperature increases. It is particularly severe for stainless steels because of tube-plugging problems due to mass transfer. Adamson et al. (Ref 38) conducted corrosion tests in a thermal convection loop involving 43.5KF-10.9NaF-44.5LiF-1.1UF_4 (mol%) with an 815 °C (1500 °F) hot leg and a 704 °C (1300 °F) cold leg. Types 410, 430, 316, 310, and 347 suffered severe tube-plugging problems at the cold leg within short test durations. Nickel and nickel-base alloys, on the other hand, showed no plugging even after 500 h of testing. However, these alloys suffered corrosion at the hot leg after 500 h of exposure. Alloy 600 suffered internal attack consisting of voids about 0.30 to 0.38 mm (12 to 15 mils) deep. Nimonic alloy 75 suffered intergranular pitting about 0.20 to 0.33 mm (8 to 13 mils) deep, and nickel suffered even metal removal of about 0.23 mm (9 mils).

Misra and Whittenberger (Ref 39) reported corrosion data for a variety of commercial alloys in molten LiF-19.5CaF_2, which was being considered for a heat-storage medium in an advanced solar space power system, at 797 °C (1467 °F) for 500 h. The tests were conducted in alumina crucibles with argon as a cover gas. Results are tabulated in Table 15.11. For nickel-base alloys, chromium was detrimental. No influence of chromium, however, was noted on iron-base alloys.

Molten fluorides are generally used in a closed system under vacuum or an inert atmosphere. However, hydrogen fluoride may be present in the system, resulting in increased corrosion rates. Moisture, a common impurity in fluoride salts, can react with fluorides to produce gaseous HF (Ref 39), some of which may dissolve in the melt. Corrosion by HF will also be involved, leading to production of hydrogen (Ref 39). Therefore, it is important to reduce the moisture level in the salt to reduce corrosion attack (Ref 39).

15.7 Corrosion in Molten Carbonates

Molten carbonates are generally less corrosive than molten chlorides or hydroxides. Coyle et al. (Ref 9) evaluated three different molten salts for a possible heat-transfer and energy-storage medium capable of operating 900 °C (1650 °F) for a solar power generation system. Both the eutectic sodium-potassium-magnesium chloride (33NaCl-21.5KCl-45.5$MgCl_2$, mol%) and the sodium hydroxide were found to be too corrosive for many commercial alloys. The eutectic sodium-potassium carbonate (58Na_2CO_3-42K_2CO_3, mol%), on the other hand, showed promise because of the much lower corrosion rates exhibited by many commercial alloys. Corrosion data generated in molten carbonate salt at 900 °C (1650 °F) for 504 h are summarized in Table 15.12. The best performer was Ni-Cr-Fe-Mo alloy (alloy X), followed by Ni-Cr-Fe-Al alloy (alloy 214) and Co-Ni-Cr-W alloy (alloy 188). The Ni-Cr-Mo

Table 15.11 Results of corrosion tests in LiF-19.5CaF_2 at 797 °C (1467 °F) for 500 h

	Depth of attack, μm (mils)	
Alloy	General(a)	Grain boundary(b)
Mild steel	…	155 (6.1)
304	…	185 (7.3)
310	…	130 (5.1)
316	…	165 (6.5)
RA330	…	270 (10.6)
B	30 (1.2)	…
N	15 (0.6)	15 (0.6)
S	90 (3.5)	…
X	…	140 (5.5)
600	90 (3.5)	30 (1.2)
718	45 (1.8)	120 (4.7)
75	30 (1.2)	135 (5.3)
25	…	95 (3.7)
188	…	105 (4.1)

Tests were conducted in alumina crucibles under argon. (a) Intragranular voids near surface. (b) Intergranular voids. Source: Ref 39

alloy (alloy S) was severely corroded. No evidence of a systematic trend for the correlation between alloying elements and performance is noted. A significant difference in corrosion was observed between two samples of alloy 800 obtained from different suppliers. However, two samples of alloy 600 showed good agreement.

At lower temperatures, molten carbonate corrosion generally becomes less severe. In molten eutectic alkali metal carbonate, Grantham et al. (Ref 40) found that many commercial alloys, including Types 304L, 310, and 347, and alloys 600, C, N, X, and 25, exhibited low corrosion rates (about 0.01mg/cm^2/h or less) at 600 °C (1110 °F). Nonoxidizing N_2 was used for the cover gas in their corrosion tests, which may also have contributed to low corrosion rates. The temperature dependence of corrosion rate can also be seen in the results generated by Grantham and Ferry (Ref 41) in the eutectic Li_2CO_3-Na_2CO_3-K_2CO_3 (about equal weight) at 500, 600, and 700 °C (930, 1110, and 1290 °F). The cover gas in this case was not reported. Corrosion rates were found to be less than 0.025, 0.025, and 2.54 mm/yr (1, 1, and 100 mpy) at 500, 600, and 700 °C (930, 1110, and 1290 °F), respectively.

15.8 Summary

The corrosion behavior of alloys in molten chlorides, nitrates/nitrites, sodium hydroxide, fluorides, and carbonates was reviewed. In general, corrosion rates of metals and alloys are strongly dependent on temperature and can generally be reduced by decreasing the temperature. Reducing oxidizing impurities, such as oxygen and water vapor, in the melt can also significantly reduce the corrosiveness of the molten salt. Thermal gradients in the melt, in the case of circulating systems, may cause dissolution of an alloying element at the hot leg and deposition of that element at the cold leg, leading to potential tube-plugging problems.

Table 15.12 Results of corrosion tests in molten eutectic sodium-potassium carbonate at 900 °C (1650 °F) for 504 h

Alloy	Total depth of attack(a), mm (mils)
X	0.12 (4.7)
214	0.19 (7.5)
188	0.22 (8.7)
556	0.26 (10.2)
X-750	0.27 (10.6)
600(b)	0.34 (13.4)
600(b)	0.44 (17.3)
R-41	0.42 (16.5)
N	0.51 (20.1)
304SS	0.54 (21.3)
316SS	0.63 (24.8)
230	0.77 (30.3)
Nickel	>0.30 (11.8)
800(b)	0.25 (9.8)
800(b)	>0.8 (31.5)
S	>1.43 (56.3)

N_2-0.1CO_2-(1–10O_2) was used for the cover gas. (a) All alloys showed metal loss only except nickel, which suffered 0.2 mm (7.9 mils) metal loss and more than 0.11 mm (4.3 mils) intergranular attack. (b) Two samples from two different suppliers. Source: Ref 9

Corrosion data generated from different chloride salts at temperatures ranging from 400 to 900 °C (750 to 1650 °F) for various cast and wrought alloys were presented. The data are rather limited and fail to show a definitive correlation between alloying elements and performance. Intergranular attack is the major corrosion morphology in molten chlorides. Cold work may significantly accelerate intergranular attack. If the cold work effect is confirmed to be a general phenomenon in molten chloride salts, annealing of fabricated components prior to service is recommended.

The corrosion behavior of commercial alloys in molten $NaNO_3$-KNO_3 is reasonably well understood. For applications at temperatures up to 630 °C (1170 °F), many commercial alloys, including austenitic stainless steels, are capable of handling the molten salt. At higher temperatures, nickel-base alloys are preferred because of the increased salt corrosivity. The resistance of alloys to molten $NaNO_3$-KNO_3 improves with increasing nickel content. Nickel, however, performed poorly.

Corrosion data related to molten sodium hydroxide (caustic soda) are rather limited. At 900 °C (1650 °F), the salt is probably too corrosive for metallic materials to handle. Metals and alloys may have adequate resistance to molten sodium hydroxide at 680 °C (1260 °F) and lower temperatures. Nickel, particularly low-carbon nickel such as Ni201, is most resistant to the molten salt. Corrosion rates can be significantly increased under dynamic conditions.

Corrosion of alloys in molten fluorides has been extensively studied for nuclear reactor applications. A nickel-base alloy, Hastelloy alloy N, has been found to be most suitable in molten fluoride salts. Since molten fluorides are used in a circulating system with temperature differentials, mass transfer induced corrosion due to thermal gradients in the loop becomes an important issue. It creates the potential for tube fouling

and plugging at the cold leg of the loop. Stainless steels are generally worse than nickel and nickel-base alloys in terms of tube-plugging problems.

Molten carbonates are generally less corrosive than molten chlorides or hydroxides. Some of the alloys that perform best in molten eutectic Na_2CO_3-K_2CO_3 at high temperatures such as 900 °C (1650 °F) include Ni-Cr-Fe-Mo alloy (alloy X), Ni-Cr-Fe-Al alloy (alloy 214), and Co-Ni-Cr-W alloy (alloy 188).

REFERENCES

1. D.G. Lovering, in *Molten Salt Technology,* D.G. Lovering, Ed., Plenum Press, 1982, p 1
2. G.J. Janz and R.P.T. Tomkins, *Corrosion,* Vol 35 (No. 11), 1979, p 485
3. J.W. Koger, in *Corrosion,* Vol 13, 9th ed., Metals Handbook, ASM International, 1987, p 51
4. J.W. Koger and S.L. Pohlman, in *Corrosion,* Vol 13, 9th ed., Metals Handbook, ASM International, 1987, p 88
5. A. Rahmel, in *Molten Salt Technology,* D.G. Lovering, Ed., Plenum Press, 1982, p 265
6. J.H. Jackson and M.H. LaChance, *Trans. ASM,* Vol 46, 1954, p 157
7. G.Y. Lai, M.F. Rothman, and D.E. Fluck, Paper No. 14, *Corrosion/85,* NACE, 1985
8. G.Y. Lai, unpublished results, Haynes International, Inc., 1986
9. R.T. Coyle, T.M. Thomas, and G.Y. Lai, in *High Temperature Corrosion in Energy Systems,* M.F. Rothman, Ed., The Metallurgical Society of AIME, 1985, p 627
10. H. Susskind, F.B. Hill, L. Green, S. Kalish, L. Kukacka, W.E. McNulty, and E. Wirsing, *Chem. Eng. Prog.,* Vol 56 (No. 3), 1960, p 57
11. J.E. Battles, F.C. Mrazek, W.D. Tuohig, and K.M. Myles, in *Corrosion Problems in Energy Conversion and Generation,* C.S. Tedmon, Jr., Ed., The Electrochemical Society, 1974, p 20
12. K. Takehara and T. Ueshiba, *J. Soc. Mater. Sci. Jpn.,* Vol 179, 1968, p 755
13. S.K. Srivastava, unpublished results, Haynes International, Inc., 1989
14. G.Y. Lai, unpublished results, Haynes International, Inc., 1989
15. R.W. Bradshaw, "Thermal Convection Loop Corrosion Tests of Type 316SS and Alloy 800 in Molten Nitrate Salts," SAND 81-8210, Sandia Laboratory, Livermore, CA, Feb 1982
16. P.F. Tortorelli and J.E. DeVan, "Thermal Convection Loop Study of the Corrosion of Fe-Ni-Cr Alloys by Molten $NaNO_3$-KNO_3," ORNL TM-8298, Oak Ridge National Laboratory, Oak Ridge, TN, Dec 1982
17. R.W. Bradshaw, "A Thermal Convection Loop Study of Corrosion of Alloy 800 in Molten $NaNO_3$-KNO_3," SAND 82-8911, Sandia Laboratory, Livermore, CA, Jan 1983
18. R.W. Bradshaw, "Kinetic Oxidation and Elemental Depletion of Austenitic and Ferritic Steels in Molten Nitrate Salt," SAND 87-8011, Sandia Laboratory, Livermore, CA, 1987
19. R.W. Bradshaw, "Oxidation of Chromium-Molybdenum Steels by Molten Sodium Nitrate-Potassium Nitrate," SAND 87-8012, Sandia Laboratory, Livermore, CA 1987
20. R.W. Carling, R.W. Bradshaw, and R.W. Mar, *J. Mater. Energy Sys.,* Vol 4 (No. 4), 1983, p 229
21. R.W. Bradshaw, "Oxidation and Chromium Depletion of Alloy 800 and Type 316SS in Molten $NaNO_3$-KNO_3 at Temperatures above 600 °C," SAND 86-9009, Sandia Laboratory, Livermore, CA, Jan 1987
22. R.W. Bradshaw and R.W. Carling, "A Review of the Chemical and Physical Properties of Molten Alkali Nitrate Salts and Their Effect on Materials Used for Solar Central Receivers," SAND 87-8005, Sandia Laboratory, Livermore, CA, April 1987
23. J.W. Slusser, J.B. Titcomb, M.T. Heffelfinger, and B.R. Dunbobbin, *J. Met.,* July 1985, p 24
24. D.R. Boehme and R.W. Bradshaw, *High Temp. Sci.,* Vol 18, 1984, p 39
25. G.P. Smith, "Corrosion of Materials in Fused Hydroxides," USAEC Report ORNL-2048, March 1956
26. C.M. Craighead, L.A. Smith, and R.I. Jaffee, "Screening Tests on Metals and Alloys in Contact with Sodium Hydroxide at 1000 and 1500 °F," USAEC Report BMI-705, Nov 1951
27. E.M. Simmons, N.E. Miller, J.H. Stang, and C. Weaver, "Corrosion and Components Studies on Systems Containing Fused NaOH," USAEC Report BMI-1118, July 1956
28. R.A. Lad and S.L. Simon, A Study of Corrosion and Mass Transfer of Nickel by

Molten Sodium Hydroxide, *Corrosion,* Vol 10 (No. 12), 1954, p 435
29. J.N. Gregory, N. Hodge, and J.V.G. Iredale, "The Static Corrosion of Nickel and Other Materials in Molten Caustic Soda," AERE-C/M-272, Atomic Energy Research Establishment, Harwell, U.K., March 1956
30. R.R. Miller, "Thermal Properties of Sodium Hydroxide and Lithium Metal," Quarterly Progress Report May 1–Aug 1, 1952, NRL-3230-201/52, 1952
31. G.P. Smith and E.E. Hoffman, *Corrosion,* Vol 13, 1957, p 627t
32. J.N. Gregory, N. Hodge, and J.V.G. Iredale, "The Corrosion and Erosion of Nickel by Molten Caustic Soda and Sodium Uranate Suspensions under Dynamic Conditions," AERE Report C/M 273, Atomic Energy Research Establishment, Harwell, U.K., March 1956
33. J.W. Koger, *Corrosion,* Vol 29 (No. 3), 1973, p 115
34. J.W. Koger, *Corrosion,* Vol 30 (No. 4), 1974, p 125
35. J.R. Keiser, D.L. Manning, and R.E. Clausing, in *Proc. Int. Symp. Molten Salts,* J.P. Pemsler et al., Ed., The Electrochemical Society, 1976, p 315
36. N. Iwamoto, Y. Makino, K. Furukawa, Y. Katoh, and H. Katsuta, *Trans. JWRI,* Vol 9 (No. 2), 1980, p 117
37. J.R. Keiser, J.H. DeVan, and E.J. Lawrence, *J. Nucl. Mater.,* Vol 85/86, 1979, p 295
38. G.M. Adamson, R.S. Crouse, and W.D. Manly, "Interim Report on Corrosion by Alkali-Metal Fluorides," ORNL-2337, Oak Ridge National Laboratory, Oak Ridge, TN, 1959
39. A.K. Misra and J.D. Whittenberger, "Fluoride Salts and Container materials for Thermal Energy Storage Applications in Temperature Range 973 to 1400 °K," NASA Tech. Memo. 89913, NASA Lewis Research Center, Cleveland, OH, 1987
40. L.F. Grantham, P.H. Shaw, and R.D. Oldenkamp, in *High Temperature Metallic Corrosion of Sulfur and Its Compounds,* Z.A. Foroulis, Ed., The Electrochemical Society, 1970, p 253
41. L.F. Grantham and P.B. Ferry, in *Proc. Int. Symp. Molten Salts,* J.P. Pemsler et al. Eds., The Electrochemical Society, 1976, p 270